Journal of
Ceramic Science
and Technology

J. Ceram. Sci. Tech., **03** [04] 199-210 (2012)
DOI: 10.4416/JCST2012-00023
available online at: http://www.ceramic-science.com

Electrochemically Induced Degradation of Screen-Printed Gold Thick Films

T.J. Rabbow*[1], N. Junker[2], C. Kretzschmar[1], M. Schneider[1], A. Michaelis[1, 2]

[1]Fraunhofer Institut für keramische Technologien und Systeme/Fraunhofer Institute for Ceramic Technologies and Systems, Winterbergstrasse 28, 01277 Dresden, Germany
[2]Institut für Werkstoffwissenschaft/Institute of Materials Science, TU Dresden, Helmholtzstrasse 7, 01069 Dresden, Germany

received June 20, 2012; received in revised form August 28, 2012; accepted October 2, 2012

Abstract

Gold thick films have been characterized by means of cyclic voltammetry in nitric acid and are compared with a pure gold electrode. Surface reconstruction and roughening is found for all electrodes, whereby the pure gold reference sample rapidly exhibits stationary behavior. In contrast, the screen-printed electrodes show a permanent linear increase of the gold surface area as measured by the charge densities for gold oxidation, which is connected with the dissolution of glass-ceramic compounds. Oxides of bismuth and copper and their aluminates are regularly used to adjust the morphology of thick films and to enhance the adhesion of screen-printed layers. Electrochemical reactions of both elements (Bi, Cu) are detected. An in-house produced gold paste free of these oxides was used for comparison and shows a linear increase in oxidation charge density as well. Cu and Bi compounds take part in the electrochemical reaction and accelerate the surface increase. The dissolution of glass-ceramic components from the surface and at the interface between thick film and substrate is revealed in FESEM images of the electrodes and at cross-sections. A model is set up for the electrochemically induced localized degradation of the thick films, which are attacked at the boundary layer to the electrolyte and the glass-ceramic interface between the LTCC substrate and gold layers.

Keywords: LTCC, screen printing gold paste, thick film electrode, electrochemical degradation

I. Introduction

Since the first production of a silver screen-printing paste by DuPont in 1939, thick film technologies have become well-established manufacturing methods for various industries [1]. The hybrid integration of silicon-based integrated circuits bonded to ceramic substrates applies thick films for electric connection via screen-printed conductors. Modern silicon solar cells contain front- and backside metallization as current collectors produced with screen-printed aluminum and silver [2]. Also, today electrochemical sensors for gaseous and liquid media are produced with thick film technologies [3, 4].

Each screen-printing paste is a composition of metal powders, glasses and ceramics, organic binders and additives for the rheology of the paste, which is adapted to the individual substrate and the purpose of duty. Nevertheless, the sintered thick film is often post-processed with electrochemical methods. High-efficiency solar cells contain reinforced electroplated silver metallization [2]. In microelectronics, copper or silver conductors are often bonded with electroless deposits of nickel and gold [5]. Furthermore, permanent and regular analysis especially of liquid media (e.g. drinking water monitoring) with screen-printed electrochemical sensors affords high stability of the material. The influence of paste composition or morphology of the sintered electrode has not been investigated sufficiently, literature on the influence of the thick films on electrochemical reactions is sparse [6, 7].

Thick film compositions are generally optimized for good adhesion or low contact resistance to the substrate, which is not necessarily the optimum composition for electrochemical applications. The chemical durability of binding glasses in thick films has been investigated [8] and glass compositions especially for electrochemical applications have been recently developed [9]. In the literature, no detailed information is available on the electrochemical stability of thick films or possible electrochemical degradation mechanisms. Three screen-printing pastes were selected to investigate different morphologies and compositions of thick films. These thick films are regarded as model systems that represent possible structures of thick films in order to study the influence on the electrochemical behavior. Thick films often contain Bi_2O_3 and Cu_2O to achieve good adhesion and better sintering characteristics [10, 11]. With an in-house produced paste free of these oxides, it is possible to investigate and compare their influence on stability. A pure gold electrode was used as a reference sample.

* Corresponding author: thomas.rabbow@ikts.fraunhofer.de

II. Experimental

Three different gold thick films (DuPont 5742, ESL 8837G and an in-house produced paste) and a sheet of gold (99.9 % Au, MaTeck GmbH) were polarized in 1.0 M HNO_3. Prior to the polarization treatment the sheet of gold was mechanically ground with an abrasive paper and cleaned with a piranha solution. The thick film electrodes were screen-printed in a circular shape and a conductor path onto a LTCC substrate (DuPont951) that was covered by a resin. The electrolyte solutions were prepared by means of dilution of highly concentrated nitric acid (HNO_3 65 % p.a. grade, Acros Chemicals) with deionized water. Exact concentration was achieved by means of titration control. All the materials were polarized in a three-electrode arrangement with a saturated calomel reference electrode (SCE; Sensortechnik Meinsberg GmbH, Germany) from E = -400 mV to 1700 mV for 3000 sweeps at a scan rate of 200 mVs^{-1}. The potential values in this report are given with respect to SCE. All cyclic voltammograms (CV) were measured in a separate, nitrogen-purged electrolyte solution. Afterwards the electrodes were placed again into the original electrolyte solution to keep almost the total amount of the cumulative dissolved material components over the whole treatment period. The experimental setup was realized with a PGU 20V-2A-E potentiostat (IPS, Germany). A platinized titanium extended metal (A = 1.0 cm^2) was used as the counter-electrode. All measurements were performed in a polypropylene beaker with an unstirred electrolyte (80 ml), at room temperature (23 °C) and FESEM investigations and EDX analysis were conducted in collaboration with Carl Zeiss NTS GmbH, Germany. The Au-ratio at the surface of each thick film was calculated based on analysis of FESEM images.

III. Results and Discussion

Gold is the most noble metal. Nevertheless, pre-conditioning of gold electrodes is necessary to achieve ideally reversible electrochemical processes. A simple cleaning of the electrodes is often insufficient. Different methods of combined cleaning and pre-treatment for electrochemical applications were investigated. Besides chemical cleaning, e.g. with a piranha solution or other oxidants, electrochemical methods have been successfully applied [12]. With repetitive potential cycling in acids, it is possible to obtain stationary and reproducible conditions at the surface of the electrode. Each cycle leads to a change of the crystal lattice of gold to Au_2O_3 and back to the gold at boundary layers. Especially at defect sites the crystal lattice can rearrange thereby, which is often described as reconstruction [13, 14]. Furthermore, impurities are removed by anodic oxidation, and changes of the pH with hydrogen and oxygen development at the electrode enhance the dissolution. The later effect can be regarded as a microscopic electrochemical cleaning.

For these reasons cyclic voltammetry was chosen as pretreatment as well as a characterization method for the material. Screen-printed electrodes and a pure gold sample were investigated in the range of the electrolyte stability from the cathodic hydrogen evolution reaction (E = -400 mV) to the anodic oxygen formation (E = + 1700 mV). Fig. 1 provides an overview of all measurements in the complete potential range during 3000 cycles. Differences of the thick films in comparison with the pure gold are found and will be discussed with regard to four aspects: gold oxidation, changes of the surface morphology, specific nitrate adsorption, as well as the oxidation and reduction of glass-ceramic phases that are functional components. Thick films consist of a composite material, and an influence on the electrochemical reactions and long-term stability can be expected. Changes in the morphology and microstructure are analyzed based on cross-sections and an electrochemically induced degradation mechanism is unfolded.

A sheet of pure gold (99.9 %) was used as a reference sample. The polycrystalline material exhibits a broad potential range for the gold oxidation during the first cycles (Fig. 2 bottom). At first a small peak a_2 is detected at E = 1220 mV followed by a broad peak a_3. During the first 100 cycles, permanent changes in the oxidation curve are observed and a_2 increases strongly. Thereafter an almost stationary behavior is obtained and the current density for the gold oxidation shows minimal changes between the 100th and 3000th repetition, which can be regarded as one criterion for sufficient pretreatment. According to the literature, the observed current shape in the range of a_2 and a_3 could be assigned to (210) oriented crystals in the material [15]. It is very unlikely that the polycrystalline gold sample contains a higher amount of (210) oriented grains, however, the electrochemical procedure and the adsorption of nitrate anions can increase the surface area of (210) oriented planes in a super lattice structure by reconstruction as described in literature [13, 14]. Interestingly for all thick film electrodes, a strong peak at E = 1220 mV is detected, which indicates that nitric acid prefers the formation of super lattice structures on (210) oriented planes.

The increase of the current density of the gold oxidation during the first cycles is considered as a typical behavior, which will be compared with the thick films. Three phenomena (cleaning, reconstruction and roughening) can cause the increase at the pure gold electrode. Since the surface was cleaned thoroughly and the electrode consists of 99.9 % gold, the removal of organic layers and impurities can only have a minor influence on the increasing current density. Nevertheless, the subsequent hydrogen and oxygen formation does affect the electrode. The changing pH value as well as gas formation enhance the dissolution of impurities and surface layers, which can be regarded as microscopic cleaning.

Microstructural changes of the gold boundary layer are expected to have a rather strong influence on the increasing gold oxidation peak. On the one hand the crystal lattice is permanently exchanging between Au_2O_3 and Au whereby atoms at defect sites can rearrange. A potential induced diffusion of surface atoms with the formation of super lattices structures is called reconstruction. On the other hand the increasing oxidation current density can be caused by a roughening either owing to a cavitation effect of collapsing hydrogen and oxygen or by repetitive dissolution and subsequent reduction of soluble gold nitrate. However, Shackleford [16] *et al.* showed that gold dissolution is kineti-

cally inhibited at scan rates above 10 mVs^{-1}. Nevertheless, the FESEM image of the gold sample shows strong macroscopic roughening after 3000 cycles (cf. Fig. 10), which explains the increase of the current density for the oxidation. The combination of macroscopic roughening and reconstruction leads to the increase of oxidation current density with preferred formation of super lattices on (210) oriented crystal planes. Surface cleaning and reconstruction can also be recognized from a pre-oxidation peak a_1 at a potential of E = 1000 mV, which is detected after 100 cycles (see Fig. 2, bottom). It is known that specifically adsorbed anions like sulfate or nitrate are exchanged at the surface before the gold oxidation. Peukert [17] *et al.* investigated the Au oxidation process in 0.5 M H_2SO_4 with CV and XPS studies and concluded that following equations can be derived for the oxidation process occurring within the potential range from E = 900 mV to E = 1500 mV vs. SCE:

According to Peukert *et al.*, Au_2O_3 will be formed via an intermediate AuO(OH) at higher potentials. For the discussion of the electrochemistry of thick films it is important to investigate the potential interval between E = -200 mV up to E = 800 mV (Fig. 2 top) since the oxidation of typical glass-ceramic phases can be observed. In the case of the pure gold sheet no oxidation of other metals is observed. Besides this, after approx. 2000 cycles the oxidation of hydrogen can be detected in a high amount (Fig. 2 top). The overvoltage for the hydrogen reduction at the gold electrode decreases owing to the pre-treatment procedure (compare Fig. 1), and at a sweep rate of 200 mVs^{-1} enough hydrogen is developed in front of the electrode that such a high oxidation peak is observed.

In contrast to the reference material, the gold oxidation of the thick film from DuPont (DP5742) does not become stationary (Fig. 3 bottom). As mentioned earlier, stationary behavior can be expected after approximately 100 cycles. The permanent increase of the current density therefore has to result from the specific properties of the composite material where not only reactions at the gold occur but also at glass-ceramic phases, leading to extended growth of the gold surface area. Before gold oxidation, again a pre-oxidation peak a_1 from desorption of nitrate anions is observed. In accordance with the permanent increase of gold oxidation this pre-peak also rises, which indicates the surface growth during 3000 cycles.

Table 1: Reactions of electrochemical gold oxidation

$Peak_{Fig.\ No.}$	Reaction	Equation No.
a_1	$Au{\cdot}NO^-_{3\ ad} + H_2O \rightarrow Au{\cdot}H_2O_{ad} + NO^-_3$	Eq. 1
a_2	$Au{\cdot}H_2O_{ad} + H_2O \rightarrow Au{\cdot}OH_{ad} + H_3O^+ + e^-$	Eq. 2
a_3	$Au{\cdot}OH_{ad} + 2\ H_2O \rightarrow Au(OH)_3 + 2\ H^+ + 2\ e^-$	Eq. 3

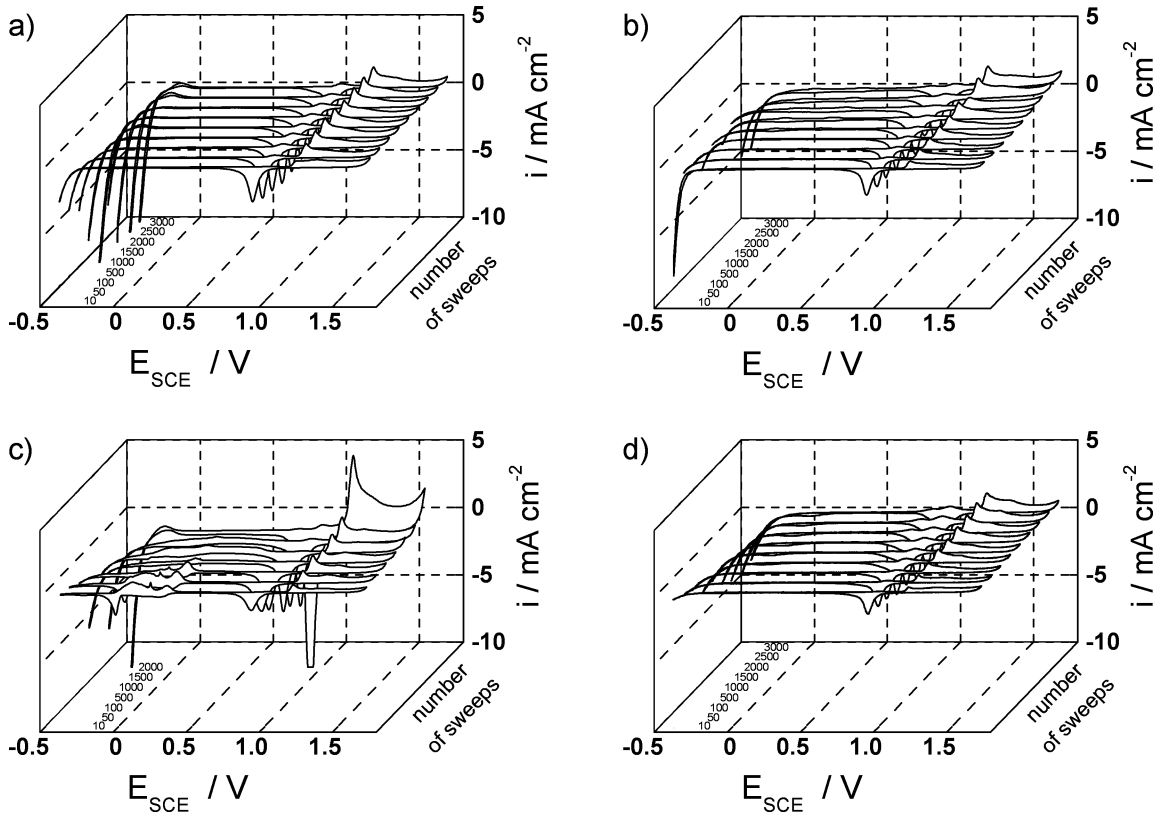

Fig. 1: Cyclic voltammograms of the investigated materials polarized vs. SCE in 1.0 M HNO_3 (a) Au(99.9%), b) DuPont 5742, c) ESL 8837G and d) IKTS with a sweep-number-dependent arrangement; initial state (front) to final state (background).

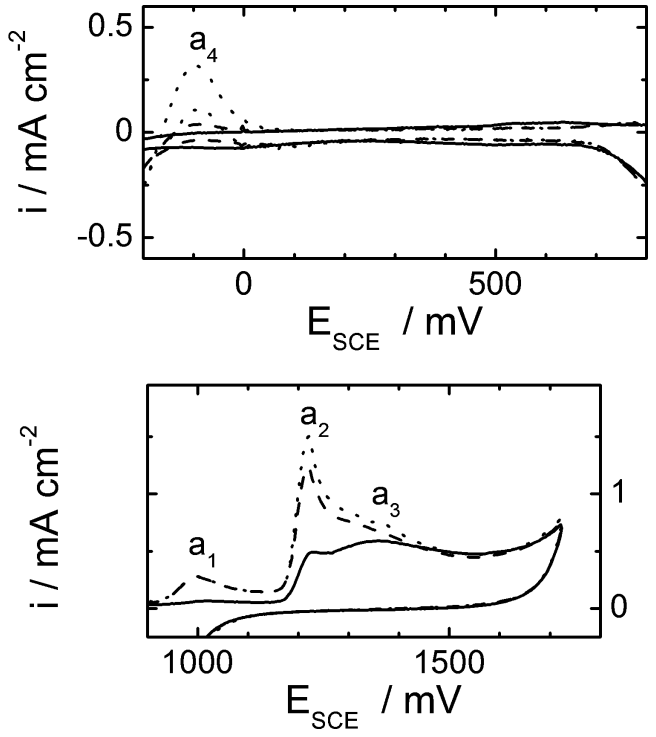

Fig. 2: CV curve sections of pure Au (99.9%) within the potential ranges from -200 mV to 800 mV (top) and from 900 mV to 1700 mV (bottom). Curves of the 10th (solid), the 1500th (dashed) and the 3000th (dotted) sweep are shown.

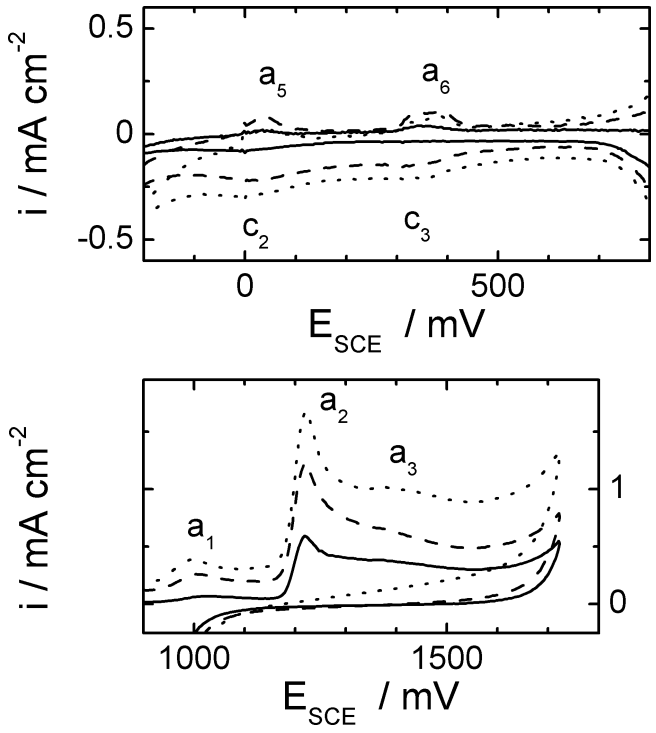

Fig. 3: CV curve sections of the DuPont 5742 thick film within the potential ranges from -200 mV to 800 mV (top) and from 900 mV to 1700 mV (bottom). Curves of the 10th (solid), the 1500th (dashed) and the 3000th (dotted) sweep are shown.

From the beginning of the first cycle up to the end of the experiment the DP5742 electrode shows one predominant oxidation peak at E = 1220 mV, which again can be explained by a high amount of (210) oriented crystal planes even though thick films are expected to be a polycrystalline material. However, during the sintering of screen-printing pastes the growth of grains and the arrangement of a typical microstructure are observed (compare Fig. 10 b, c, d). All thick films were sintered under the same conditions at 850 °C with a typical temperature routine. Gold particles will not melt below 1064 °C, but screen-printing pastes contain ceramic and glass components (e.g. Bi_2O_3, PbO) that can create a liquid phase at 850 °C, enabling a flow of gold particles inside the thick film. A sintering of gold below the melting point in combination with the flow of particles inside the glass phase generates a typical microstructure for each screen-printed paste depending on the specific composition and glass content.

In the case of the DP5742 thick film, the predominant peak at E = 1220 mV increases further during the 3000 cycles, which shows the reconstruction on (210) oriented planes similar to the pure gold sheet. Besides this, another small peak at E = 1370 mV develops, which might indicate a surface reconstruction as well on (111) oriented crystal planes. In a previous study, predominant (111) oriented crystal planes had clearly been detected at the DP5742 thick film [7]. In the meantime, the supplier has changed the composition of the paste, which is now declared as lead-free and obviously induces changes in the microstructure of the sintered electrode.

The glass-ceramic components can be detected in the second potential range (Fig. 3 top). Two oxidation (a_5, a_6) and reduction (c_2, c_3) peaks are visible in the cyclic voltammogram. According to the data sheet, DP5742 does contain Cu_2O but the exact composition of each screen-printing paste is the intellectual property of the supplier. Lead oxide had been a component formerly but the paste is meanwhile labeled as lead-free. From our measurements it can be assumed that lead oxide has been replaced with bismuth oxide, which was not detected in a previous study [7]. The strong influence of glass and ceramic phases on the microstructure can be concluded once more from this fact.

Metal oxides and glasses are used for two purposes inside thick films. One function of low temperature melting glasses like PbO (mp. 888 °C) or Bi_2O_3 (mp. 817 °C) is to establish a flow during sintering by which metal particles can rearrange. The amount and composition of these oxides strongly determines the morphology and microstructure of the sintered thick film. Furthermore these glasses establish an adhesion to the substrate, and ceramic metal oxides like Cu_2O or CuO generate a chemical binding of the thick film to the substrate based on the formation of spinel-type compounds [10,18]. LTCC mainly consists of Al_2O_3, glassy SiO_2 and various alumosilicates. During sintering, CuO forms $CuAl_2O_3$ and enhances the adhesion of the screen-printed layer.

The observation of corresponding oxidation and reduction peaks in Fig. 3 top implies that metal oxides inside the thick film can be reduced electrochemically. Therefore it becomes obvious that the oxides are in electrical contact to the gold phase and the electrolyte. From this fact the question arises via which compounds do the electrochemical reactions with Cu and Bi proceed? Copper can form $CuAl_2O_3$ (spinel-type) as well as $CuAlO_2$ (de-

lafossite-type) [19,20], bismuth will be contained as Bi_2O_3 and additionally it can form the bismuth-aluminates [21,22] $Bi_2Al_4O_9$ and $BiAlO_3$ with Al_2O_3. Furthermore Cu and Bi can be dissolved as aqueous Cu^{2+} and Bi^{3+} complexes. Possible reactions and their standard potentials [23] (as far as known) of Cu, Bi and their compounds are given in Eqs. 4 – 11.

From EDX analysis (cf. Table 3) it is known that Cu and Bi are contained inside the thick film. In comparison to the standard potential (Eqs. 4 – 11) the peak couple (a_6, c_3) at approx. E = 330 mV vs. SCE has to be identified with Cu/Cu(I) reaction. However, aqueous Cu(I) complexes are unstable but can be stabilized by anions. It can be assumed that the insertion of Cu(I) ions into a ceramic network or matrix also stabilizes this oxidation state. The formation of delafossite copper(I)-aluminate ($CuAlO_2$) during sintering can be regarded as such a matrix. During cyclic voltammetry, Cu(I) becomes reduced but the AlO(OH) network partially remains and can incorporate Cu(I) again after subsequent oxidation.

The second peak (a_5, c_2) at approx. E = 30 mV vs. SCE cannot clearly be assigned to one reaction. Compared to standard potentials Bi/Bi(III) as well as Cu/Cu(II) reactions are possible (see Eqs. 4 – 11). Bismuth as well as Copper can be oxidized to soluble Bi(III) and Cu(II) complexes. In this case a gradual decrease of the peak current density would be expected since the reduction will never be complete owing to diffusion losses. In contrast the peak current density increases firstly and remains on a constant level. Therefore Eqs. 6 and 10 are considered, where the reaction proceeds via solid state compounds of Cu and Cu(II). The dissolution of Cu(II) and Bi(III) will take place on a minor scale.

Similar to the DP5742 electrode the gold oxidation of the thick film 8837G from ESL shows a strong peak at E = 1210 mV vs. SCE indicating a predominant oxidation on (210) oriented crystals, but a small peak at E = 1370 mV is also found (Fig. 4 bottom). The consecutive potential scans lead to a strong increase of the surface size, which is displayed in rising current density for the oxidation. Again a cleaning effect due to the pre-treatment is detected from the increase of both the oxidation peaks and the pre-oxidation peak owing to the exchange of nitrate anions by water before the gold oxidation.

The increase of current density at the ESL8837G electrode is connected with strong degradation. After 2000 cycles the thick film is completely delaminated from the substrate (in Fig. 4 only the 10th and the 1500th cycles are given). After delamination the electrode was not investigated any further although the gold part retained its shape and was not dissolved. The electrochemically induced degradation hence only affects the glass-ceramic phases. In Fig. 4, top, the dissolution of glass-ceramic compounds is shown. Again reactions for Bi and Cu can be found but the current density for the oxidation and reduction is much higher in comparison to the DP5742 thick film. This electrode contains more glass-ceramic parts at the surface which become dissolved (cf. Table 1). Moreover an additional peak (a_8) is observed between the others, which could not be identified so far.

Table 2: Electrochemical redox reactions of typical compounds in thick films

$Peak_{Fig.No.}$	Reaction	Electric Potential	Equation No.
a_5	$Bi \rightarrow Bi^{3+} + e^-$	E = 0.067 V vs. SCE	Eq. 4
a_5	$Cu \rightarrow Cu^{2+} + 2\ e^-$	E = 0.099 V vs. SCE	Eq. 5
a_5	$Cu + 2\ AlO(OH) \rightarrow CuAl_2O_4 + 2\ H^+ + 2\ e^-$	E = 0.099 V vs. SCE	Eq. 6
a_6	$Cu + AlO(OH) \rightarrow CuAlO_2 + H^+ + e^-$	E = 0.280 V vs. SCE	Eq. 7
c_2	$2\ Bi + 4\ AlO(OH) + H_2O \rightarrow Bi_2Al_4O_9 + 6\ H^+ + 6\ e^-$	E = 0.067 V vs. SCE	Eq. 8
c_2	$Bi + AlO(OH) + H_2O \rightarrow BiAlO_3 + 3\ H^+ + 3\ e^-$	E = 0.067 V vs. SCE	Eq. 9
c_2	$Cu + 2\ AlO(OH) \rightarrow CuAl_2O_4 + 2\ H^+ + 2\ e^-$	E = 0.099 V vs. SCE	Eq. 10
c_3	$Cu + AlO(OH) \rightarrow CuAlO_2 + H^+ + e^-$	E = 0.280 V vs. SCE	Eq. 11

Table 3: Properties of the investigated gold electrode materials.

Electrode material	Add. included elements*)	Firing process	A_{geo} /cm^2	Au-ratio on surface /%
Au (99.9%)	-	-	0.38	100
DuPont 5742	O, Al, Si, Ca, Cu, Ag, Pb, Bi	co-fired	0.18	96
ESL 8837G	O, Al, Si, Ca, Pb, Bi	post-fired	0.10	73
IKTS	Ag	post-fired	0.18	98

*) *obtained by means of EDX analysis after firing process*

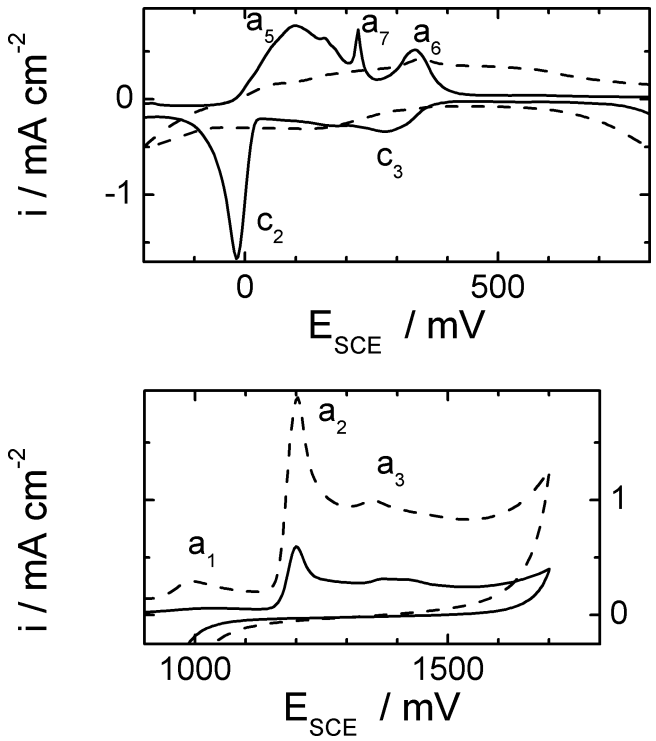

Fig. 4: CV curve sections of the ESL 8837G thick film within the potential ranges from -200 mV to 800 mV (top) and from 900 mV to 1700 mV (bottom). Curves of the 10th[h] (solid) and the 1500th (dashed) sweep are shown.

It is obvious that the rapid delamination of the ESL 8837G electrode is connected with electrochemical reactions. The oxidation peak a_7 is much broader for this electrode and it has to be assumed that in this case Bi and Cu are also dissolved as aqueous complexes, accelerating delamination. High contents of bismuth and its oxide will be dissolved electrochemically and the copper reactions between solid state compounds can only proceed if the matrix of aluminate is sufficient for higher amounts of oxidized Cu(I) and Cu(II). Owing to the strong dissolution of the glass-ceramic phase the thick film is partially delaminated, leading to a further increase of gold surface area and a diffusion of the electrolyte into the interface of substrate and thick film, which also destabilizes the adhesion by Bi and Cu compounds.

The IKTS thick film is an in-house development which is optimized to minimize glass-ceramic particles at the surface and contains no oxide of copper or bismuth. Very similar to the other thick films the current density for gold oxidation increases significantly up to the 1500th cycle and continues growing until the 3000th cycle (Fig. 5, bottom). At the pure gold electrode the current density becomes stationary after 100 cycles. Therefore this increase at the IKTS-electrode has to be assigned to changes and dissolution of the glass-ceramic phases even though this thick film is optimized to a pure gold surface. Two oxidation peaks (a_2 and a_3) are found which display (210) and (111) oriented crystal planes similar to the other thick films. The pre-oxidation peak, a_1, from desorption of the nitrate anion increases in a similar way to the oxidation peaks, which expresses the electrode cleaning and the surface growth.

Within the second potential range no oxidation of Bi or Cu compounds is found (Fig. 5, top). This is expected on the basis of the composition of the screen-printed paste. Nevertheless there is the possibility for an enrichment of glasses from the LTCC substrate inside the thick film after firing. Although the IKTS electrode does not contain Bi_2O_3 or Cu_2O, good adhesion during the experiment is achieved. From this result it can be concluded once more that the electrochemical reduction of metal oxides leads to a destabilization and can be regarded as a new degradation mechanism in addition to solely chemical dissolution. An additional reduction peak c_4 is observed at E = 0 mV vs. SCE which occurs after 1500 cycles. Since no corresponding oxidation peak is detected, the reduction of oxygen is highly presumable at this potential. All electrolytes have been nitrogen-purged before the recording of the shown cyclic voltammograms (in Figs. 2 – 5), but of course there is oxygen development above E = 1600 mV vs. SCE. It is highly presumable that oxygen becomes stored inside pores of the thick film which prevent cavities from ascending so that oxygen is available for reduction.

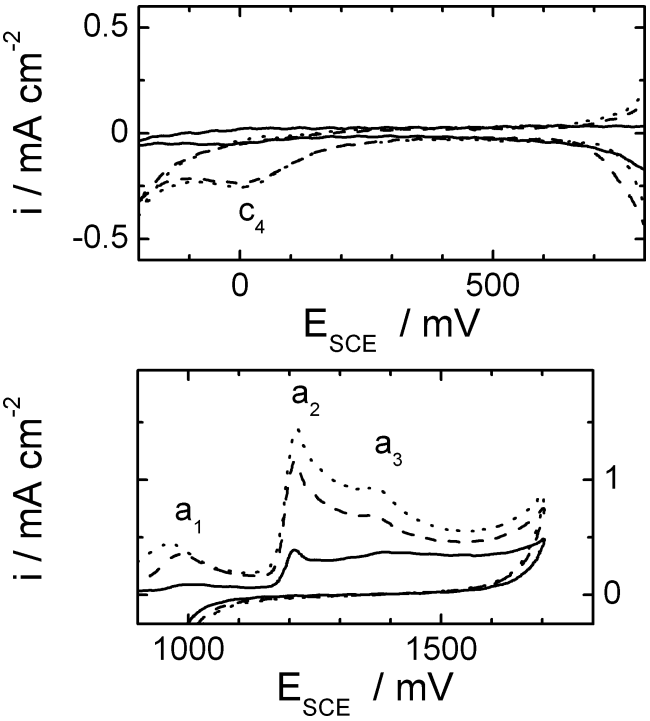

Fig. 5: CV curve sections of the IKTS thick film within the potential ranges from -200 mV to 800 mV (top) and from 900 mV to 1700 mV (bottom). Curves of the 10th (solid), the 1500th (dashed) and the 3000th (dotted) sweep are shown.

The increase of the current density for the gold oxidation can be quantified to give information about the changes of the gold surface. Gold oxidation has been applied to characterize and quantify the surface area of polycrystalline and single crystal electrodes [24]. Although the reaction has been investigated in great detail over the past 50 years [17,25–32], no final conclusion has been drawn either about stoichiometry of the formed oxide/hydroxide nor about the oxidation mechanism itself. However, this present work proceeds from the assumption that until a specific anodic potential is reached, localized at the s.c. Burshtein minimum, the electrochemical oxidation of gold only forms a monolayer of $Au(OH)_3$ on the surface. This process affords approximately a charge of

390 μCcm^{-2} for a smooth, polycrystalline gold surface [24]. For all electrodes the real surface area was estimated with this procedure. Different reasons have to be taken in account for the increase of current density.

1) Anodic and cathodic polarization as well as hydrogen and oxygen evolution will remove impurities and adhering layers from the electrode
2) The gas formation in front of the electrode – oxygen evolution in the case of anodic polarization and hydrogen evolution in the case of cathodic polarization – can cause surface roughening as a result of the implosion of cavities
3) A potential induced surface reconstruction during cyclic voltammetry can lead to an increase of surface atoms by up to 24 % as reported in the literature [13]
4) In the case of thick film electrodes, the dissolution of glassy and ceramic compounds leads to an increase in free gold surface

The pure gold electrode shows a fast rise of charge density from 0.9 mCcm^{-2} to 1.25 mCcm^{-2} within the first 100 cycles, thereafter a stationary behavior is observed (Fig. 6). Removal of impurities can only have a minor effect at the cleaned electrode since the reference sample contains 99.9 % gold. A reconstruction of the crystal planes owing to the potential scans and a roughening of the surface by developing gas cavities have to be the reason. The FE-SEM image of this electrode (Fig. 10 a, bottom) provides evidence of the strong roughening as a result of the electrochemical treatment, which has to be regarded as a typical behavior of pure gold surfaces under these conditions. It has to be assumed that the surface roughness is stationary after approximately 100 cycles.

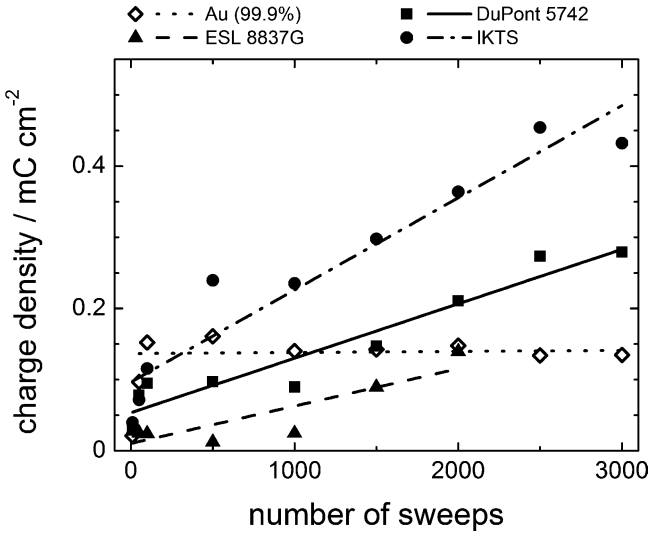

Fig. 6: Charge density for the gold oxidation during 3000 potential scans.

The development of gold oxidation charge density of thick films can be compared to the reference material. A generally different behavior is found for all thick films. Up to the 500th or 2000th cycle respectively, the gold oxidation of thick films shows a charge density well below that needed for pure gold. The thick films possess a smaller gold surface owing to their smoothness and glass-ceramic inclusions. The charge density does not become stationary. The gold oxidation proceeds with a linear increase during the potential scans. Except in the case of the ESL8837G electrode, even during the first 100 scans only a linear increase is observed at the thick films. Therefore a surface roughening or a reconstruction of crystal planes has to take place at slower time scales or is completely suppressed. Surface roughening by gas cavities could be reduced because of less hydrogen and oxygen development and crystal reconstruction might be limited because of defects at the boundary surface owing to glass-ceramic inclusions. The permanent increase of charge density for the oxidation does not occur at the pure gold and therefore it has to result from a growth of gold surface owing to dissolution of glass-ceramic material during each cycle.

A similar behavior is found for the pre-oxidation peak, which also shows a stationary charge density at the pure gold electrode but a linear increase for the thick films (Fig. 7). The peak results from the exchange of specifically adsorbed nitrate anions at the surface within the electrochemical double layer, which of course is connected to the surface size. But in comparison to oxidation charge density, a different order for the electrodes is found for the pre-oxidation peak. The highest peak is observed for the IKTS electrode which exhibits the smallest gold charge density of the thick films. The specific adsorption of anions is strongly depending on the crystal orientation. Even though a similar oxidation peak was found for the three different thick films, it has to be assumed that many more nitrate anions are adsorbed at the IKTS electrode owing to appropriate crystal planes.

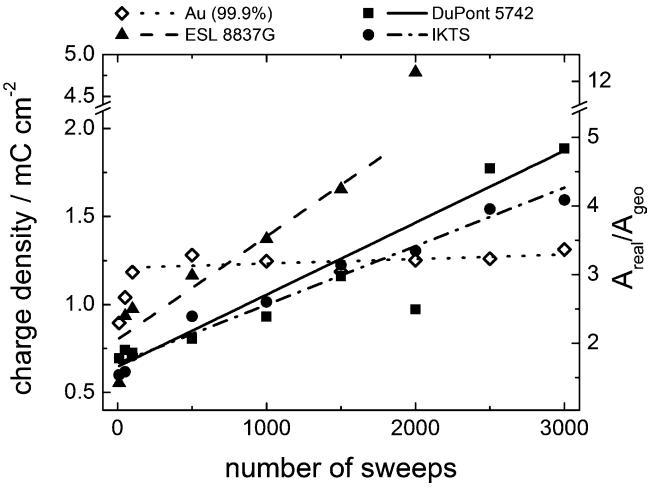

Fig. 7: Charge density of the pre-oxidation peak during 3000 potential scans.

To find a reason for the increase of gold oxidation charge density at the thick films, the oxidation and reduction peaks a_5, a_6 and c_2, c_3 are analyzed (Figs. 8, 9). As shown by cyclic voltammetry and by EDX, the IKTS electrode does not contain any copper or bismuth. Nevertheless, a linear increase of the gold oxidation charge density is also observed, which results from the dissolution of glasses and ceramics at the surface and at the interface binding the metal/substrate. This can be regarded as basic dissolution behavior which is induced by the electrochemical reaction even if the thick film does not contain elements that can be reduced or oxidized. ESL and DuPont thick films contain to some extent copper and bismuth oxides

and aluminates which take part in the electrochemical reaction. In Fig. 6 it becomes obvious that these thick films show a faster increase of charge density which displays a faster degradation. Both the ESL and DuPont thick film shows reactions of copper and bismuth, however, the temporal development is different. The oxidation and reduction of copper and bismuth increases at the DuPont thick film during the 500th to 1500th scan but remains constant on a higher level (Fig. 8). At the ESL thick film the reaction rates are reversed, decreasing from high charge densities to a low level. As mentioned before, this is connected with a delamination of the gold layer in which all Cu and Bi components are finally removed from the thick film. It is obvious to suggest that the strong reaction at the ESL electrode leads to the dissolution of glass-ceramic Cu- and Bi-containing phases, inducing the delamination. In contrast to this the stationary charge densities at the DuPont electrode have to be explained by reactions between solid state compounds without a significant release of Cu and Bi ions into the electrolyte.

The development of charge densities for gold oxidation (Fig. 6) and for dissolution of copper and bismuth (Fig. 8, 9) has to be explained by changes on the surface of the gold or at the interface to the ceramic substrate. All electrodes have been analyzed by FESEM before and after the electrochemical measurements to correlate the increase of oxidation current density and dissolution of glass-ceramic compounds with changes of the morphology. The pure gold sheet (Fig. 10a, left) shows scratches from polishing before the experiment. Severe roughness is observed after 3000 polarization cycles (Fig. 10a, right), which causes the increase of current density for gold oxidation.

The thick film from DuPont (Fig. 10 b) is characterized by sharp-edged steps and a terrace structure which indicate the presence of predominant oriented crystals as detected by specific peaks in the cyclic voltammogram. Ceramic inclusions are visible between gold grains. Image analysis reveals a portion of 4 % ceramic particles at the surface before the measurements. During the potential scans a permanent oxidation and reduction of metal oxides was observed, which increased slightly up to the 3000th cycle. The FESEM image shows that the inclusions are no longer present. Severe roughening comparable to that of the pure gold electrode is not observed.

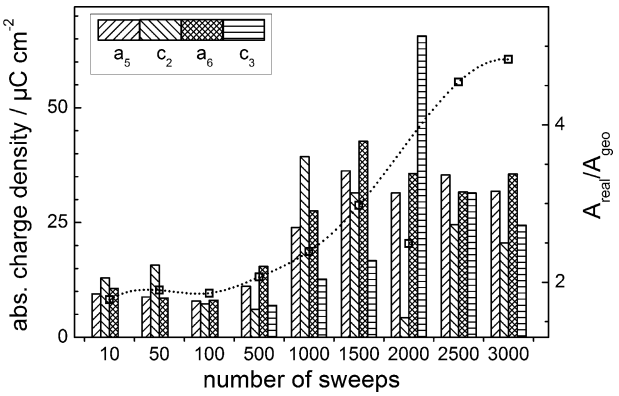

Fig. 8: Charge densities of the redox-processes of Bi and Cu containing glass-ceramic phase of DuPont 5742 thick film. Dotted line shows the ratio between A_{real} and A_{geo} (cf. Fig. 6).

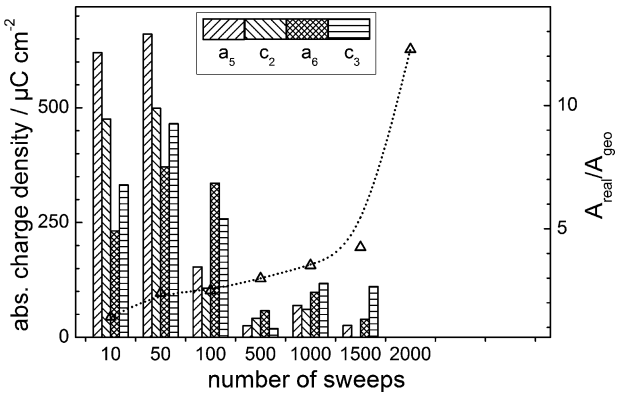

Fig. 9: Charge densities of the redox-processes of Bi and Cu containing glass-ceramic phase of ESL 8837G thick film. Dotted line shows the ratio between A_{real} and A_{geo} (cf. Fig. 6).

The ESL thick film has a porous morphology with small inclusions and broad domains where the surface is covered with a glass-ceramic phase. Owing to the high amount of boundary surface between gold and glass-ceramic phase in the initial state, it is obvious that the dissolution of Cu and Bi proceeds at high charge densities from the beginning. After polarization the gold surface is roughened on selected grains whereas others remain smooth. A similar behavior is found for the IKTS electrode. Before the electrochemical procedure a polycrystalline microstructure is found with smooth grains but some pores. The polarization in nitric acid causes severe roughening on some grains of thick film which presumably possess crystal orientations that easily generate reconstructed surfaces.

Nevertheless from these FESEM images it cannot be understood why there is a constant oxidation and reduction reaction of Cu and Bi at the DuPont electrode. After 3000 cycles the surface contains far fewer ceramic inclusions than was initially the case. Moreover, no pores or severe roughening on the surface is found which could increase the real surface area after dissolution of inclusions. The electrochemical reaction can be regarded as a cleaning procedure in this case. Cross-sections of the interface between gold thick film and ceramic substrate were analyzed to explain the permanent growth of the gold surface area and constant oxidation and reduction charge density for Cu and Bi (Figs. 11 and 12). Initially the gold thick film is attached via a closed interface to the glass-ceramic substrate (Fig. 11). After 3000 polarization cycles a clear gap between the thick film and the glass-ceramic phase from LTCC substrate is found. Inclusions from the surface of the thick film are apparently dissolved. Therefore it is possible that glass-ceramic compounds at the interface can also be dissolved by the electrochemical reaction as shown by the cross-section. Thus the electrolyte reaches more gold boundary surface, which explains the increase of the gold oxidation charge density. Moreover it becomes clear why a constant Cu and Bi reaction is observed. Inside the gap very little electrolyte is exchanged whereby oxidized compounds can be reduced without losses due to diffusion.

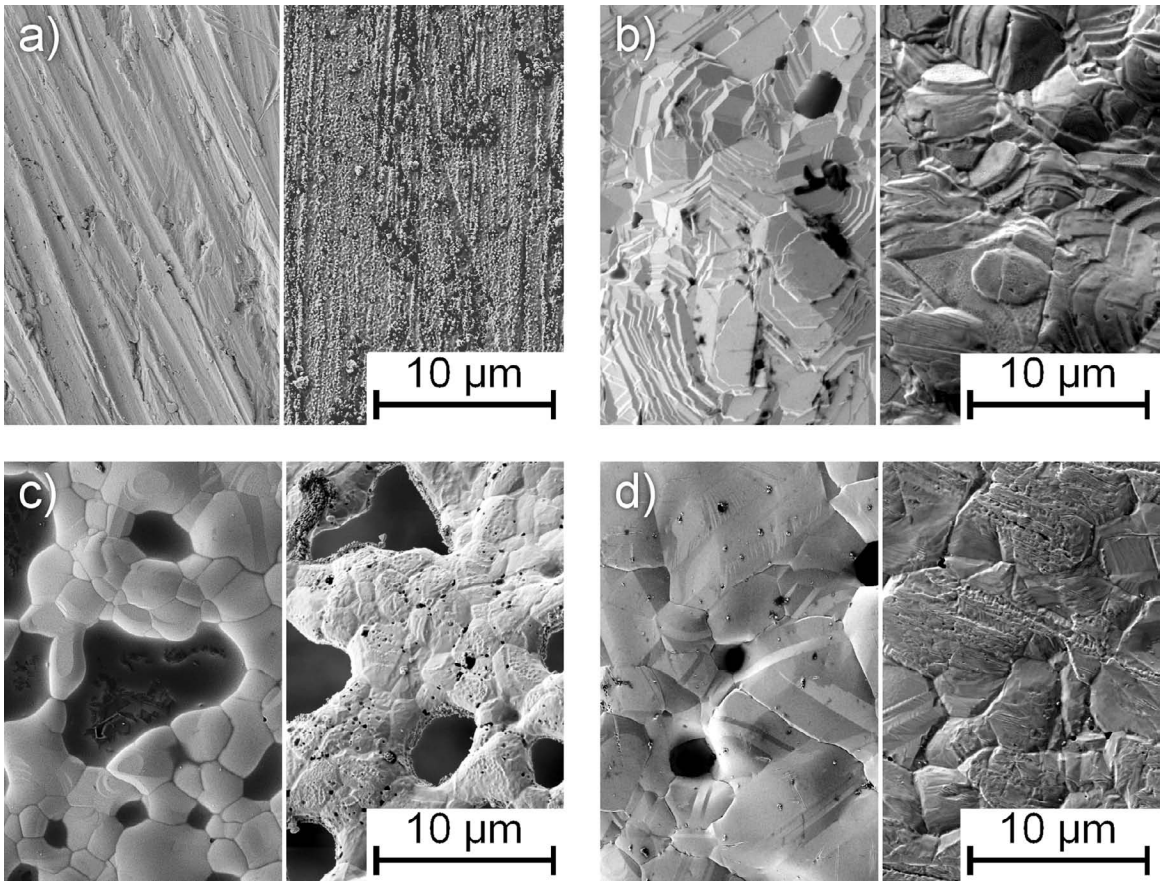

Fig. 10: FESEM images of initial surface and after electrochemical reaction a) pure gold and the thick films b) DuPont 5742, c) ESL 8837G and d) IKTS.

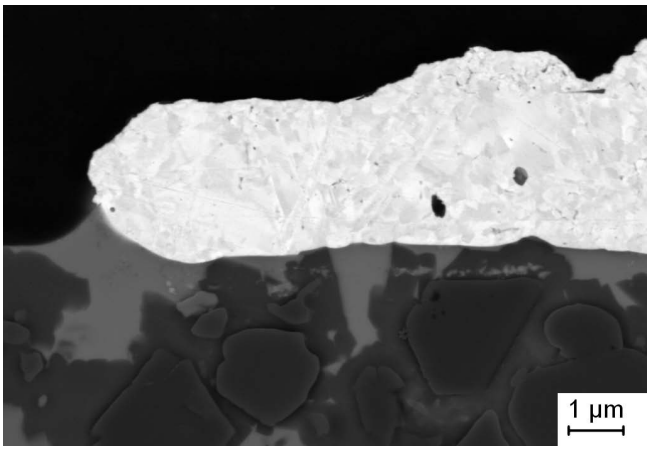

Fig. 11: FESEM cross-section of the initial interface between the DuPont thick film and the ceramic substrate.

The experimental observations allow us to set up a model for the degradation of thick films. FESEM and EDX analysis show that copper and bismuth are contained inside glass-ceramic inclusions between the gold grains and at the interface to the substrate. The electrochemical measurement verifies that both metals take part at the reaction and therefore are in a conductive contact between the gold and electrolyte. The electrochemical dissolution involves the following steps as schematically shown in Fig. 13. During anodic sweep, elemental copper and bismuth contents of the thick films are oxidized, can diffuse into the electrolyte and are replaced by protons (Fig. 13 – (2)). Furthermore water becomes electrolyzed at higher potentials, which leads to a further increase of protons at the surface (Fig. 13 – (3)). The glass-ceramic matrix is attacked by the generated protons and is partially dissolved. During the reduction of Cu (in spinel or delafossite-type aluminates) aluminum-oxy-hydroxide is formed in accordance with Eqs. 6 and 7, which further enhances the dissolution of the matrix (Fig. 13 – (4)). Similarly aluminum-oxy-hydroxide formation can be supposed for bismuth-aluminates (Eqs. 8 and 9). In the following anodic sweep, copper and bismuth can be oxidized and dissolved correspondingly. At lower potentials protons are reduced to hydrogen gas, leading to a local increase of the pH value whereby the glass-ceramic matrix can be dissolved in the case of very high hydrogen development. By repetition of anodic and cathodic polarization the matrix is dissolved. The FESEM images show that inclusions are removed at the surface and a gap between substrate and thick film is formed at the interface. The oxidation of Cu and Bi must not necessarily lead to aqueous dissolution of metals with depletion of the glass-ceramic phase. As mentioned above, both metals could also be oxidized and reduced to solid state components. Nevertheless the generation of high proton concentration and the electrochemically induced formation of aluminum-oxy-hydroxides will lead to dissolution of the glass-ceramic matrix. Four resulting degradation effects by electrochemical treatment are summarized in Fig. 13 – (6).

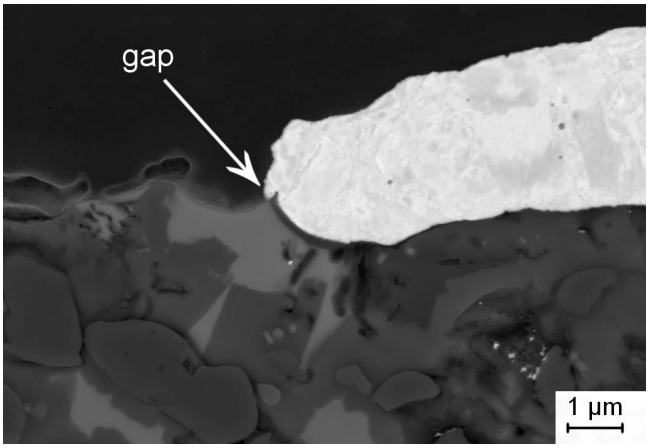

Fig. 12: FESEM cross-section of the interface at the DuPont thick film after the electrochemical reaction.

1. The dissolution of the glass-ceramic anchor of the thick film will cause its delamination as observed for the ESL thick film.
2. The gold surface is roughened.
3. Removal of glass-ceramic inclusions on the surface.
4. Removal of glass-ceramic inclusions within the material via channels along the grain boundaries. This would explain the side-by-side increase in the real surface area with the charge of Cu and Bi redox reactions observed at the DuPont thick film (Fig. 8).

Conclusion

The stability of three different thick films has been tested in an acidic medium under the influence of repeated anodic and cathodic polarization and compared with a pure gold electrode. The investigated thick films are regarded as model electrodes that represent three different possible surface morphologies, compositions and therefore exhibit different electrochemical behavior and stability.

The gold electrodes are pre-conditioned and cleaned by means of the electrochemical procedure. Surface reconstruction and roughening cause an increase in surface area. A stationary charge density is observed after approx. 100 cycles at the pure gold sheet. In contrast, the oxidation charge density shows a linear increase for all thick films. Reconstruction and roughening are also found at certain grains of the screen-printed electrodes but the permanent growth of gold surface is mainly caused by dissolution of glass-ceramic phase as a result of electrochemical treatment. The oxidation charge density provides a quantitative measure to characterize the gradual degradation. Two electrodes contain copper and bismuth oxides and aluminates, which are oxidized and reduced electrochemically. Since the third thick film is free of these elements but also exhibits a linear increase of oxidation charge density, the main electrochemical degradation proceeds via the dissolution of the glass-ceramic matrix but can be enhanced by compounds that take part in the electrochemical reaction. Glass-ceramic phases are dissolved from the surface of the thick film, and from FESEM images of cross-sections it can be concluded that the main dissolution takes place at the interface to the substrate. A strong dissolution leads to the delamination of the screen-printed film as observed at one electrode with a high boundary surface. In this case very strong Cu and Bi reactions are detected until complete depletion. The degradation obviously depends strongly on the morphology of the electrode and compact, closed thick films are preferred for better durability in harsh media and under these polarization conditions.

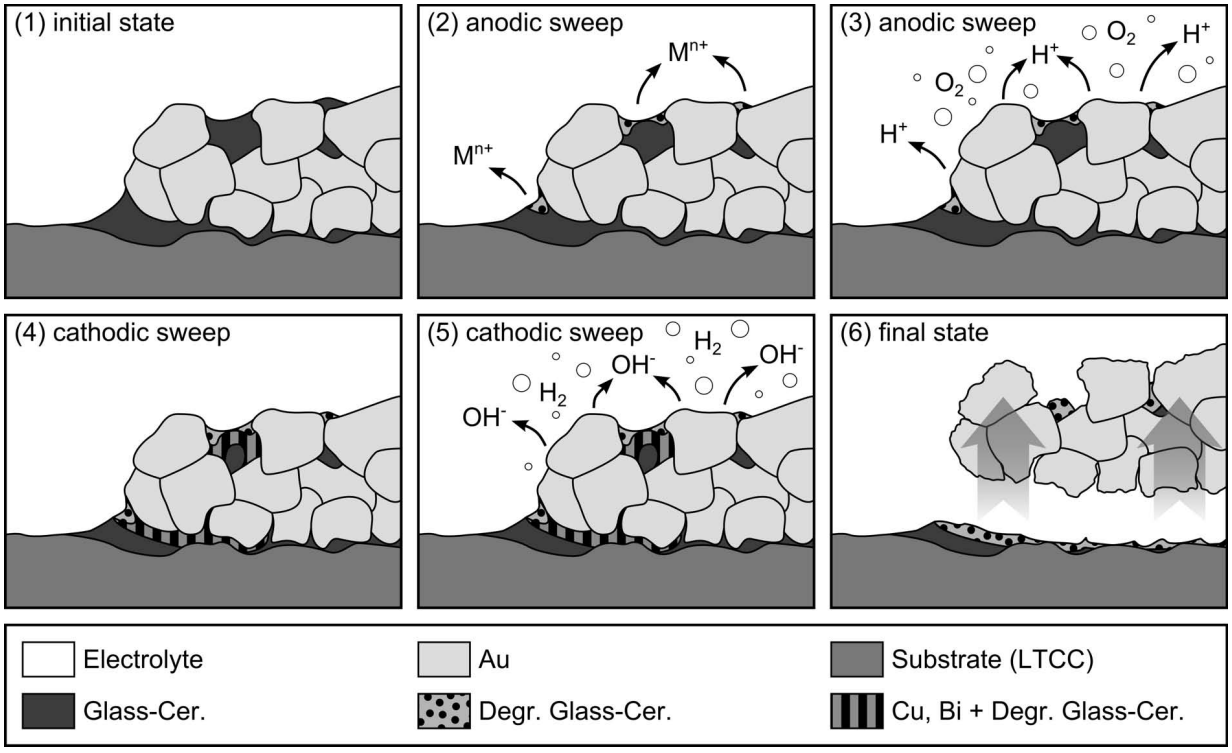

Fig. 13: Schematic drawing of the electrochemically induced thick film degradation.

It could be shown that under polarization very localized dissolution processes occur which can be regarded as an electrochemically induced degradation mechanism. Furthermore it becomes possible with electrochemical measurements to observe gradual changes at the electrodes as a result of degradation.

Acknowledgment

The financial support by the DFG in the project "Elektrochemisches Verhalten und Degradation von siebgedruckten Metall-Keramik-Werkstoffverbunden" ("Electrochemical behavior and degradation of screen-printed metal-ceramic material composites" MI509/11 – 1, SCHN745/8 – 1) is gratefully acknowledged.

References

1 Ménil, F., Debéda, H., Lucat, C.: Screen-printed thick-films: from materials to functional devices, *J. Eur. Ceram. Soc.,* **25**, 2105 – 2113, (2005).

2 2. Pysch, D., Mette, A., Filipovic, A., Glunz, S.W.: Comprehensive analysis of advanced solar cell contacts consisting of printed fine-line seed layers thickened by silver plating, *Prog. Photovoltaics: Research and Applications*, **17,** 101, (2009).

3 Park, C.O., Akbar, S.A.: Ceramics for Chemical Sensing, *J. Mater. Sci.*, **38**, 4611 – 4637, (2003).

4 Goldbach, M., Axthelm, H., Keusgen, M.: LTCC-based microchips for the electrochemical detection of phenolic compounds, *Sensor Actuat. B-Chem.*, **120**, 346, (2006).

5 Johannessen, R., Oldervoll, F., Strisland, F.: High temperature reliability of aluminium wire-bonds to thin film, thick film and low temperature co-fired ceramic (LTCC) substrate metallization, *Microelectron. Reliab.,* **48**, 1711 – 1719, (2008).

6 Gongora-Rubio, M.R., Fontes, M.B.A., Mendes da Rocha, Z., Richter, E.M., Angnes, L.: LTCC manifold for heavy metal detection system in biomedical and environmental fluids, *Sensor Actuat. B-Chem.*, **103**, 468, (2004).

7 Rabbow, T.J., Junker, N., Schneider, M., Michaelis, A.: Screen-printed gold thick films for electrochemical sensor applications, *Materialwiss. Werkst.*, **42**, 777, (2011).

8 Mattox, D.M., Robinson, J.: Chemical durability of lead-oxide-based, thick-film binder glasses, *J. Am. Ceram. Soc.,* **80**, 1189 – 1192, (1997).

9 http://www.imaps.org/membership/CorpBulletin/archives/-2007/2007sept4.htm

10 Imanaka, Y.: Multilayered low temperature cofired ceramics (LTCC) technology, Springer (2005).

11 Buchanan, R.C.: Ceramic materials for electronics, Marcel Dekker Inc., New York, 2nd Ed. (1991).

12 Fischer, L.M., Tenje, M., Heiskanen, A.R., Masuda, N., Castillo, J., Bentien, A., Émneus, J., Jakobsen, M.H., Boisen, A.: Gold cleaning methods for electrochemical detection applications, *Microelec. Eng.,* **86**, 1282 – 1285, (2009).

13 Gao, X., Edens, G.J., Hamelin, A., Weaver, M.J.: Real-space formation and dissipation mechanisms of hexagonal reconstruction on Au(100) in aqueous media as explored by potentiodynamic scanning tunneling microscopy, *Surf. Sci.*, **296**, 333, (1993).

14 Hamelin, A.: Behaviour of au (100) in perchloric and sulphuric acid solutions, *J. Electroanal. Chem.*, **255**, 281, (1988).

15 Silva, F., Sottomayor, M.J., Martins, A.: Study of electrochemical properties of Au(210) face electrode in nitrate solutions, *Electrochim. Acta*, **39**, 491, (1994).

16 Shackleford, S.G.D., Boxalla, C., Porta, S.N., Taylor, R.J.: An *In Situ* electrochemical quartz crystal microbalance study of polycrystalline gold electrodes in nitric acid solution, *J. Electroanal. Chem.*, **109**, 538 – 539, (2002).

17 Peuckert, M., Coenen, F.P., Bonzel, H.P.: On the surface oxidation of a gold electrode in 1 N H_2SO_4 electrolyte, *Surf. Sci.*, **141**, 515, (1984).

18 Kadota, S., Shibata, K.: Gold conductor pastes for high density circuit, *Electrocomp. Sci. Tech.*, **9**, 31 – 41, (1981).

19 Ishiguro, T., Kitazawa, A., Mizutani, N., Kato, M.: Single-crystal growth and crystal structure refinement of $CuAlO_2$, *J. Solid State Chem.*, **40**, 170, (1981).

20 Paulsson, H., Rosén, E.: A study of the formation of $CuAl_2O_4$ from CuO and Al_2O_3 by solid state reaction at 1000 °C and 950 °C, *Z. Anorg. Allg. Chem.*, **401**, 172, (1973).

21 MacKenzie, K.J.D., Dougherty, T., Barrel, J.: The electronic properties of complex oxides of bismuth with the mullite structure, *J. Eur. Ceram. Soc.*, **28**, 499 – 504, (2008).

22 Bloom, I., Hash, M.C., Zebrowski, J.P., Myles, K.M., Krumpel, M.: Oxide-ion conductivity of bismuth aluminates, *Solid State Ionics*, **53 – 56**, 739 – 747, (1992).

23 Lide, D.R.: CRC Handbook of chemistry and physics, CRC Press, Boca Raton, 73rd edition, (1992).

24 Trasatti, S., Petrii, O. A.: Real surface area measurements in electrochemistry, *Pure Appl. Chem.*, **63**, 711, (1991).

25 Laitinen, H.A., Chao, M.S.: The anodic surface oxidation of gold, *J. Electrochem. Soc.*, **108**, 726, (1961).

26 Brummer, S.B., Makrides, A.C.: Surface oxidation of gold electrodes, *J. Electrochem. Soc.*, **111,** 1122, (1964).

27 Dickinson, T., Povey, A.F., Sherwood, P.M.A.: X-ray photoelectron spectroscopic studies of oxide films on platinum and gold electrodes, *J. Chem. Soc. Faraday T.,* **71,** 298, (1975).

28 Angerstein-Kozlowska, H., Conway, B.E., Hamelin, A., Stoicoviciu, L.: Elementary steps of electrochemical oxidation of single-crystal planes of au - I. chemical basis of processes involving geometry of anions and the electrode surfaces, *Electrochim. Acta*, **31**, 1051 – 1061, (1986).

29 Š;trbac, S., Adžić, R.R., Hamelin, A.: Oxide formation on gold single crystal stepped surfaces, *J. Electroanal. Chem.*, **249**, 291, (1988).

30 Cahan, B.D., Villullas, H.M., Yeager, E.B.: The effects of trace anions on the voltammetry of single crystal gold surfaces, *J. Electroanal. Chem.*, **306**, 213, (1991).

31 Hamelin, A.: Cyclic voltammetry at gold single-crystal Surfaces. part 1. behaviour at low-index faces, *J. Electroanal. Chem.*, **407,** 1, (1996).

32 Juodkazis, K., Juodkazyt, J., Šebeka, B., Lukinskas, A.: Cyclic voltammetric studies on the reduction of a gold oxide surface layer, *Electrochem. Comm.*, **1**, 315, (1999).